Eur Biophys J (1991) 19:157–168

European Biophysics Journal

Mean-field and Monte Carlo simulation studies of the lateral distribution of proteins in membranes

Maria M. Sperotto and Ole G. Mouritsen

Department of Structural Properties of Materials, The Technical University of Denmark, Building 307, DK-2800 Lyngby, Denmark

Received July 9, 1990/Accepted October 16, 1990

Abstract. Monte Carlo simulations and mean-field calculations have been applied to a statistical mechanical lattice model of lipid-protein interactions in membranes in order to investigate the phase equilibria as well as the state of aggregation of small integral membrane proteins in dipalmitoyl phosphatidylcholine bilayers. The model, which provides a detailed description of the pure lipid bilayer phase transition, incorporates hydrophobic matching between the lipid and protein hydrophobic thicknesses as a major contribution to the lipid-protein interactions. The model is analyzed in the regime of low protein concentration. It is found that a large mismatch between the lipid and protein hydrophobic thicknesses does not guarantee protein aggregation even though it strongly affects the phase behaviour. This result is consistent with experimental work (Lewis and Engelman 1983) considering the effect of lipid acyl-chain length on the planar organization of bacteriorhodopsin in fluid phospholipid bilayers. The model calculations predict that the lipid-mediated formation of protein aggregates in the membrane plane is mainly controlled by the strength of the direct lipid-protein hydrophobic attractive interaction but that direct protein-protein interactions are needed to induce substantial aggregation.

Key words: Lipid-protein interactions – Phase transition – Lipid bilayer – Hydropobic thickness – Protein aggregation – Monte Carlo simulation – Mean-field theory

Introduction

The modern view of the membrane structure is based on the so-called 'fluid-mosaic' model of Singer and Nicolson (1972), which describes the membrane as a fluid-mosaic pseudo-two-dimensional aggregate of a lipid bilayer with embedded integral proteins. Both proteins and lipid molecules are supposed to be free to move in the 'mosaic' plane. Furthermore, as stressed by Singer and Nicolson themselves, "a prediction of the fluid mosaic model is that the two-dimensional long-range distribution of any integral protein in the plane of the membrane is essentially random." Therefore, the model does not account for the existence of large-scale inhomogeneities in the lateral distribution of the membrane components, which may contribute – together with the short-range inhomogeneities – to the functional specialization of membrane regions (Quinn and Chapman 1980; Sanderman 1978; McElhaney 1982; Carruthers and Melchior 1986; Sackmann 1984) by affecting the enzymatic and physiological function of specific regions. The lateral inhomogeneity in the distribution of the membrane components has a 'static' as well as a 'dynamic' component which are consequences of the cooperativity of the membrane system. The formation of long-lived bacteriorhodopsin 'patches' found in the purple membrane of halophile bacteria (Stoeckenius et al. 1979) is an example of the static large-scale ($\sim 10^4$ Å) inhomogeneity in the protein lateral distribution. However, the lateral mobility of many membrane proteins can also cause the existence of short-lived small-scale (100–1000 Å) inhomogeneities that may reflect the existence of enzymatic pathways (Metzger and Ishizaka 1982).

The various levels of inhomogeneities in the protein distribution in lipid membranes involve, for example, protein aggregation, phase separation, and protein segregation and crystallization. From the point of view of equilibrium thermodynamics, these various levels proceed from a local microscopic scale to a global macroscopic scale. Phase separation and bulk protein segregation/crystallization are macroscopic phenomena, which indicate the coexistence of two macroscopically distinct phases in the lipid-protein system. Protein aggregation, on the other hand, corresponds to formation of a new type of microscopic or mesoscopic super-particle or complex consisting of a cluster of proteins which, in general, will be associated with a certain size distribution. The present paper will mainly focus on protein aggregation and protein-induced lipid phase separation.

Offprint requests to: O. G. Mouritsen

In the past, different theories have been proposed in an attempt to explain the determinants of protein aggregation in lipid membranes (Abney and Owicki 1985). In some early work, Marčelja (1976) proposed a theory based on the assumption that the driving force for the formation of protein aggregates is lipid-mediated. When two proteins come close enough to produce an overlap between the lipid regions they have perturbed, a lipid-mediated force will start to act between them. Marčelja estimated the strength of the force between two isolated proteins separated by a distance Δ_{PP}. From the knowledge of the system free energy as a function of Δ_{PP}, he calculated the protein pair-potential, $V_M(\Delta_{PP})$, and from this the effective force acting on the protein pair. It should be stressed here that the pair-potential of Marčelja is determined solely by the enthalpic part of the free energy. The theory does not account for the fact that at finite temperatures, when proteins are free to move in the membrane plane, the disordering effect of the entropy will work against an attractive interaction between proteins, thus tending to keep them in a random dispersion in order to minimize the total free energy of the system. The actual protein lateral distribution is a result of these competing effects. Therefore, to consider protein aggregation to be caused by an 'effective potential' does not give reliable information about the actual physical mechanisms from which they are generated.

According to Barion and colaborators (Barion et al. 1979) protein aggregates may be influenced by the formation of short-lifetime defects – the so-called 'holes', corresponding to temporarily unoccupied phospholipid sites – which, due to thermodynamic fluctuations in the system, occur simultaneously in the vicinity of two neighbouring proteins, thus inducing stable binding. The phenomenon depends on the protein concentration: in order to bind two proteins in a stable manner via van der Waals forces, the formation of vacancies has to involve a large number of phospholipids simultaneously. This is probably a rare event in biological membranes.

Other authors (Pearson et al. 1983; Braun et al. 1987; Abney et al. 1987) have attempted to obtain information regarding the forces acting between the proteins in aggregates using statistical mechanical methods to analyse the positional correlation of proteins in micrographs from freeze-fracture electron microscopy experiments (see Abney and Owicki 1985). The intermolecular potentials calculated by these methods contain contributions from both the enthalpic and the entropic part of the free energy, and, as in the case of the pair-potential of Marčelja, it is not possible to discern their contributions to the free energy.

The present work presents the results of a systematic theoretical model study of the lateral distribution of proteins in dipalmitoyl phosphatidylcholine (DPPC) bilayers. The aim of the work is to isolate – with the help of a lipid-protein interaction model – the relevant factors responsible for protein aggregation in membranes, and, in particular, to investigate whether the existence of a mismatch between lipid and protein hydrophobic thicknesses may significantly influence aggregation. Earlier systematic experimental studies (Riegler and Möhwald 1986; Peschke et al. 1987), as well as theoretical calculations (Mouritsen and Bloom 1984; Sperotto and Mouritsen 1988; Sperotto et al. 1989), have pointed out the importance of the mismatch between protein and lipid hydrophobic thicknesses for the phase behaviour of lipid-protein mixtures. Here, a microscopic lipid-protein interaction model is presented in order to investigate how a mismatch interaction influences the microscopic behaviour of the lipid-protein mixture. The phase equilibria of the model are determined by approximate mean-field calculations. The determination of the thermodynamic properties of the model proceeds by the use of the Monte Carlo computer-simulation techniques (Mouritsen 1990) which take proper account of the thermal density fluctuations which are important near the main bilayer phase transition (Mouritsen 1990). The computer simulations permit direct inspection of the membrane configurations on the molecular level and they therefore allow for a direct determination of the state of protein aggregation.

Microscopic model

We have adopted the ten-state model of the lipid bilayer main phase transition proposed by Pink and collaborators (Pink et al. 1980; Caillé et al. 1980). The ten-state model has previously also been used for studies of lipid-protein interactions using a set of fitted lipid-protein interaction constants (Pink and Chapman 1979; Lookman et al. 1982; Tessier-Lavigne et al. 1982; Caillé et al. 1980; Pink 1984; MacDonald and Pink 1987; Pink and Hamboyan 1990). Here, we incorporate the lipid-protein interactions into the ten-state model in the spirit of the mattress model (Mouritsen and Bloom 1984) by identifying part of the lipid-protein interaction constants in terms of molecular properties, specifically hydrophobic thickness and hydrophobic matching between the lipid and protein hydrophobic thicknesses. This type of extended model has recently been used to calculate lipid order-parameter profiles near isolated integral membrane proteins (Sperotto and Mouritsen 1990).

Pink's ten-state model (Pink et al. 1980) provides a rather accurate description of the pure lipid bilayer phase behaviour and the associated lipid-density fluctuations since it accounts for the most important conformational acyl-chain states of the lipids as well as their mutual interactions and statistics. Within this model the bilayer is considered as two monolayer sheets which are independent of each other, and each monolayer is represented by a triangular lattice. The model is a pseudo-two-dimensional lattice model which neglects the translational modes of the lipid molecules and focusses on the conformational degrees of freedom of the acyl chains. Each acyl chain can take on one of ten conformational states m, each of which is characterized by an internal energy E_m, a hydrocarbon chain length d_m, and a degeneracy D_m, which accounts for the number of conformations that have the same area A_m and same energy E_m, where $m = 1, 2, \ldots 10$. The ten states are derivable from the all-*trans* state in terms of *trans*-gauche isomerism. The state $m = 1$ is the non-degenerate gel-like ground state, representing

the all-*trans* conformation, while the state $m=10$ is a highly degenerate excited state being characteristic of the melted or fluid phase. The eight intermediate states are gel-like states containing kink and jogs excitations satisfying the requirement of low conformational energy and optimal packing. The conformational energies E_m are obtained from the energy needed for a gauche rotation (0.45×10^{-13} erg) relative to the all-*trans* conformation. The values of D_m are determined by combinatorial considerations (Caillé et al. 1980). The chain cross-sectional areas, A_m, are trivially related to the values of d_m since the volume of an acyl chain is approximately invariant under temperature changes (Marčelja 1974; Träuble and Haynes 1971). The saturated hydrocarbon chains are coupled by nearest-neighbour anisotropic forces which represent both van der Waals and steric interactions. The interactions are formulated in terms of products of shape-dependent nematic factors. The lattice approximation automatically accounts for the excluded volume effects and, to a rough approximation, for the part of the interaction with water which allows for the bilayer existence. An effective lateral pressure, Π, is added to the model to assure bilayer stability (Marčelja 1974). The Hamiltonian energy of the pure lipid bilayer model may then be written

$$\mathscr{H}_{\text{pure}}=\sum_i\sum_m (E_m+\Pi A_m)\,\mathscr{L}_{m,i} - \frac{J_0}{2}\sum_{\langle i,j\rangle}\sum_{m,n} I(d_m,d_n)\,\mathscr{L}_{m,i}\,\mathscr{L}_{n,i}\,, \tag{1}$$

where J_0 is the strength of the van der Waals interaction between neighbouring chains, and $I(d_m, d_n)$ is an interaction matrix which involves both distance and shape dependence. The Hamiltonian is expressed in terms of site occupation variables $\mathscr{L}_{m,i}$: $\mathscr{L}_{m,i}=1$ if the chain on site i is in state m, otherwise $\mathscr{L}_{m,i}=0$. The model parameters J_0 and Π are chosen in order to reproduce the transition temperature for a pure DPPC bilayer: $J_0=0.70985\times10^{-13}$ erg and $\Pi=30$ dyn cm^{-1} (Mouritsen et al. 1983).

The lipid-protein interactions are included in the model, Eq. (1), by assuming that the hydrophobic membrane spanning part of the protein molecule is a stiff, rod-like, and hydrophobically smooth object with no appreciable internal flexibility. This assumption holds in those cases where the protein structure is known, and it is normally used in protein modelling (Jähnig 1981; Sadler and Worcester 1982; Sadler et al. 1984). In this way the protein is characterized only by a cross sectional area A_P (or circumference ϱ_P) and the half-length of the hydrophobic core, d_P. In the following, the term 'protein length' will refer to d_P which is then to be compared with the hydrophobic thickness of half a bilayer. It will furthermore be assumed that the protein is small and only occupies one site of the lipid lattice.

The total Hamiltonian of the model is now

$$\mathscr{H}=\mathscr{H}_{\text{pure}}+\mathscr{H}_{\text{L-P}} \tag{2}$$

$$\mathscr{H}_{\text{L-P}}=\Pi A_P\sum_i L_{P,i}+\gamma_{\text{mis}}\left(\frac{\varrho_P}{z}\right)\sum_{\langle i,j\rangle}\sum_m |d_{m,i}-d_{P,j}|\,L_{P,j} - v_{\text{vdW}}\left(\frac{\varrho_P}{z}\right)\sum_{\langle i,j\rangle}\sum_m \min(d_{m,i},d_{P,j})\,\mathscr{L}_{m,i}\,L_{P,j}\,,$$

where z is the coordination number ($z=6$) and $L_{P,i}$ is the protein occupation variable. $\mathscr{L}_{m,i}$ and $L_{P,i}$ satisfy the comleteness relation $\sum_m \mathscr{L}_{m,i}+L_{P,i}=1$. The parameter v_{vdW} is related to the direct lipid-protein hydrophobic van der Waals-like interaction which is associated with the interfacial contact of the two species. The parameter γ_{mis} is related to the hydrophobic effect. The corresponding term in the Hamiltonian accounts for a possible existence of a *mismatch* between the protein and the lipid hydrophobic lengths. Since both of the lipid-protein interaction terms in Eq. (2) contain a factor which involves the lipid-chain length variable, $d_{m,i}$, the strength of these terms are not only determined by the interaction constants, γ_{mis} and v_{vdW}, but it depends implicitly on the temperature via the actual lipid-bilayer thickness.

The choice of the values of the lipid-protein interaction parameters γ_{mis} and v_{vdW} has been guided by the phenomenological model calculations by Sperotto and Mouritsen (1988). It is not expected, however, that the parameters of the microscopic and phenomenological models should necessarily be the same. In contrast to the phenomenological model, the microscopic model described in this article automatically includes the elastic contribution to the free energy of the bilayer, as given by a finite area compressibility. Since the hydrophobicity of typical protein side chains is half of that of the lipid hydrocarbon chains (Tanford 1973), the value of the parameter γ_{mis} in Eq. (2) depends on whether the protein length or the bilayer thickness is the larger. Specifically, the mismatch interaction parameter is approximately twice as large in the case $d_{m,i}>d_P$ as in the case $d_{m,i}<d_P$. The parameter v_{vdW} is considered to be phase independent since the lipid hydrophobic length is consistently determined by the cooperativity of the microscopic model. In this respect, the phenomenological mattress-model approach (Mouritsen and Bloom 1984), which requires the pure lipid bilayer thicknesses of the two phases as an input, is conceptually different from the microscopic approach. Hence the microscopic model contains only two model parameters which in principle are unknown and in practice are determined empirically by drawing upon the phenomenological mattress model (Mouritsen and Bloom 1984).

Calculational techniques

Monte Carlo simulation techniques (Pink 1984; Mouritsen 1990) within the canonical ensemble are applied to the microscopic model, Eq. (2), in order to study the equilibrium lateral distribution of single-site proteins free to move on the lattice during the simulations. The thermal equilibrium is provided by a combination of Glauber and Kawasaki dynamics. According to the Glauber dynamics, the lipid chains are fixed at their lattice sites but they can change their conformational state. By Kawasaki pair exchange, a lipid chain and a neighbouring protein molecule can exchange lattice sites.

In order to assess the state of protein aggregation on the lattice, the protein cluster-size distribution function,

$N(S)$, is calculated from an ensemble of typical equilibrium configurations. As a consequence of the protein lateral mobility in the lipid matrix, phase separation may occur in the system. This will influence the lateral distribution of the proteins. Since it is rather difficult to determine unambiguously the thermodynamic phase of a system from a Monte Carlo simulation within the canonical ensemble, the mean-field approximation has been used to calculate the free energy of the model. From the mean-field free energy an approximate phase diagram can be derived, which is then used as a guide for the interpretation of the $N(S)$-data obtained from the simulations. The consistency between the Monte Carlo simulation data and the mean-field phase diagram has been checked in each case considered. The mean-field theory for the present model is developed in the Appendix.

In order to understand the influence of the mismatch interaction energy term in Eq. (2) on the phase equilibria of the system and on the protein lateral distribution in each phase, different matching conditions, i.e. different protein hydrophobic lengths, d_P, (with $d_{10} < d_P < d_1$), have been considered. Furthermore, for a given choice of d_P, the influence on the system thermodynamics of the van der Waals-like interaction energy term in Eq. (2) is studied by varying the lipid-protein interaction parameter v_{vdW}.

Results

As a useful reference for the following presentation and discussion of the computer-simulation results we show in Fig. 1 the temperature variation of the hydrophobic thickness for pure DPPC bilayers as predicted by the ten-state Pink model. The figure reveals the dramatic change in thickness at the transition temperature. Considering this dramatic change one may anticipate that the mismatch interaction is going to be a main determinant of the phase equilibria of the lipid-protein membrane.

We then turn to present the results of a systematic study of the phase behaviour of different lipid-protein mixtures and the degree of aggregation of small proteins in the various phases and phase coexistence regions of these mixtures. Six representative cases are discussed, which differ from one another in the different choices of the protein hydrophobic length, d_P, and the lipid-protein van der Waals-like interaction parameter v_{vdW}. The mismatch interaction parameter is the same for all cases, $\gamma_{mis} = 0.01 \times 10^{-13}$ erg Å^{-2}.

For each of the six cases the phase diagram is described and discussed together with the results from the protein cluster size analysis. Only a few selected temperatures are considered corresponding to different parts of the phase diagram above, below, and close to the pure lipid bilayer transition temperature, T_m ($T_m = 314$ K for DPPC): $T_1 = 295$ K, $T_2 = 313$ K and $T_3 = 335$ K. The equilibrium distribution function, $N(S)$, is calculated from Monte Carlo simulations performed mostly on a lattice with 40×40 sites, 80 of which are occupied by single-site proteins. The corresponding molar protein concentration is $c_P = 0.095$. Some larger lattices have also been considered in order to estimate finite-size effects (Mouritsen 1990). Snapshots of typical microconfigurations are shown which, together with the phase diagrams, facilitate the interpretation of the simulation data.

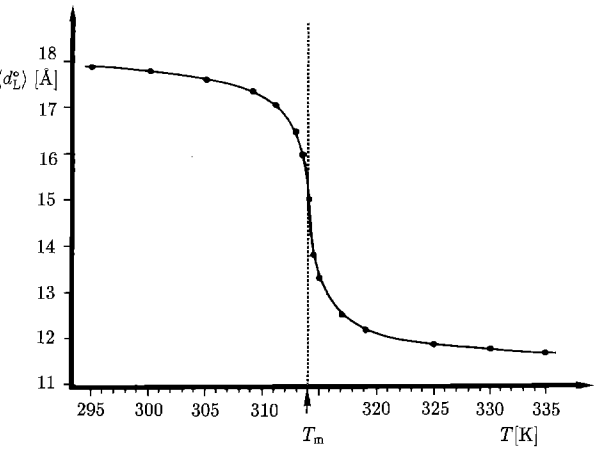

Fig. 1. Temperature dependence of the equilibrium lipid chain length, $\langle d_L^0 \rangle$, of the unperturbed DPPC bilayer. The transition temperature is $T_m = 314$ K

Case A: $d_P = 12$ Å, $v_{vdW} = 0$ (Figs. 2–4)

The phase diagram in Fig. 2 shows that massive phase separation occurs below T_m. In the phase separated region, the proteins are dissolved almost exclusively in the fluid-like regions of the bilayer. This is due to the fact that the protein length is closely matched to the fluid bilayer thickness, cf. Fig. 1, and solution of proteins in the gel phase would be very costly. However, since the attractive interaction between the lipids and the proteins is very low, the solubility of the protein is also low in the fluid phase, and therefore, one would expect a tendency for protein aggregation within the coexistence region at low temperatures where the entropy is low.

These expectations are confirmed by the results from the simulations. At $T = T_1$, for the chosen protein concentration $c_P = 0.095$, the system is in the phase separation region. The cluster-size distribution function in Fig. 3a shows that the number of isolated proteins is low and large protein aggregates are formed. That the protein aggregates appear almost exclusively in the fluid region of the lattice is demonstrated by the snapshot of Fig. 3b. As the temperature is raised toward T_2, the system leaves the phase separation region. The proteins are no longer dissolved only in a limited region and the number of isolated proteins increases strongly, as can be seen from Fig. 4a. A number of small protein aggregates remains at the temperature just above the pure lipid transition temperature. At $T = T_3$, the entropy effect only allows a small number of protein dimers and trimers still to be present in the system, as shown in Fig. 4b.

Simulations have also been performed in the case of $d_P = 15$ Å and 18 Å for the same interaction constant $v_{vdW} = 0$. The results regarding the protein distribution are similar to the those for $d_P = 12$ Å.

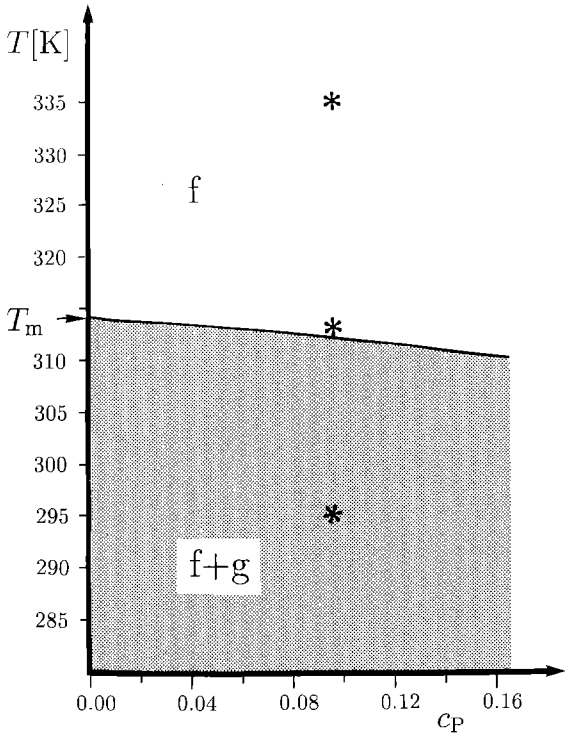

Fig. 2. *Case A:* Phase diagram in temperature, T, vs. protein concentration, c_P, for a mixture of lipids and single-site proteins with a hydrophobic length of 12 Å. The lipid-protein interaction parameters are $\gamma_{mis}=0.01\times10^{-13}$ erg Å^{-2}, and $v_{vdW}=0$. $T_m=314$ K is the transition temperature of the pure lipid bilayer. The labels f and g refer to the fluid and gel lipid phases and the shaded region $f+g$ indicates the fluid-gel coexistence region. The points indicated by * denote the points in the phase diagram investigated by computer simulation calculations

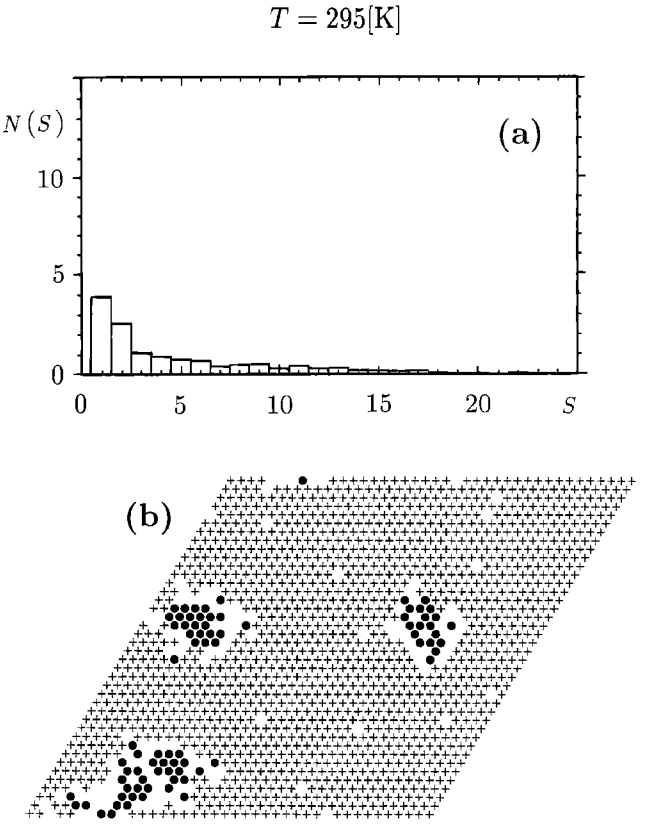

Fig. 3. *Case A* (**a**): Protein cluster size distribution on a lattice of 40×40 sites, 80 of which are single-site protein-like impurities with a hydrophobic length of 12 Å. The data are given for the temperature $T_1=295$ K. The lipid-protein interaction parameters are $\gamma_{mis}=0.01\times10^{-13}$ erg Å^{-2} and $v_{vdW}=0$. (**b**) Snapshot of a typical microconfiguration of the lattice at T_1. The proteins are indicated by dots, and gel and fluid lipid regions are denoted by grey and white areas, respectively

Case B: $d_P=12$ Å, $v_{vdW}=0.005\times10^{-13}$ erg Å^{-2} (Figs. 5, 6)

A weak attractive interaction between lipid chains and proteins is now operative, but the phase behaviour of the system does not change substantially compared to *Case A*. The phase diagram has a massive phase separation region, where the phase boundary between the fluid phase and the coexistence region is close to the one in Fig. 2 and the phase boundary between the gel phase and the coexistence region has only moved insignificantly away from the vertical axis relative to Fig. 2. For temperatures below T_m, the proteins dissolve mainly in the fluid phase-separated regions of the bilayer. At T_1 for $c_P=0.095$, the solubility in the gel phase is rather low corresponding to approximately $c_P^g=0.002$. The protein concentration in the phase separated fluid regions is almost the same as in *Case A*.

The microscopic behaviour of the system is illustrated in Fig. 5 a and b. A substantial change compared to *Case A* (Fig. 3 a and b) is seen to have taken place regarding the protein aggregation within the fluid part of the phase separation region of the bilayer below T_m. Figure 5 a shows that the proteins in this case aggregate in smaller clusters as supported by the snapshot shown in Fig. 5 b.

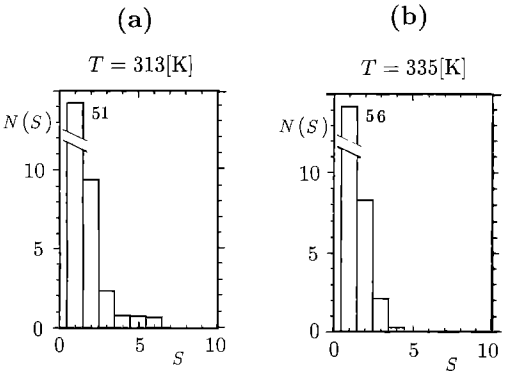

Fig. 4. *Case A:* Protein cluster size distribution on a lattice of 40×40 sites, 80 of which are single-site protein-like impurities with a hydrophobic length of 12 Å. The number indicated at the broken column in the diagram at $S=1$ denotes the number of isolated proteins. The data are given for the temperatures $T_2=313$ K (**a**) and $T_3=335$ (**b**). The lipid-protein interaction parameters are $\gamma_{mis}=0.01\times10^{-13}$ erg Å^{-2} and $v_{vdW}=0$

At T_3 the system is safely in the fluid phase and Fig. 6 a and b shows that the protein aggregation state is more polydisperse than in *Case A*. AT T_2 the system is in the fluid phase just above the two phase region. The protein distribution considerably less polydisperse than at T_3.

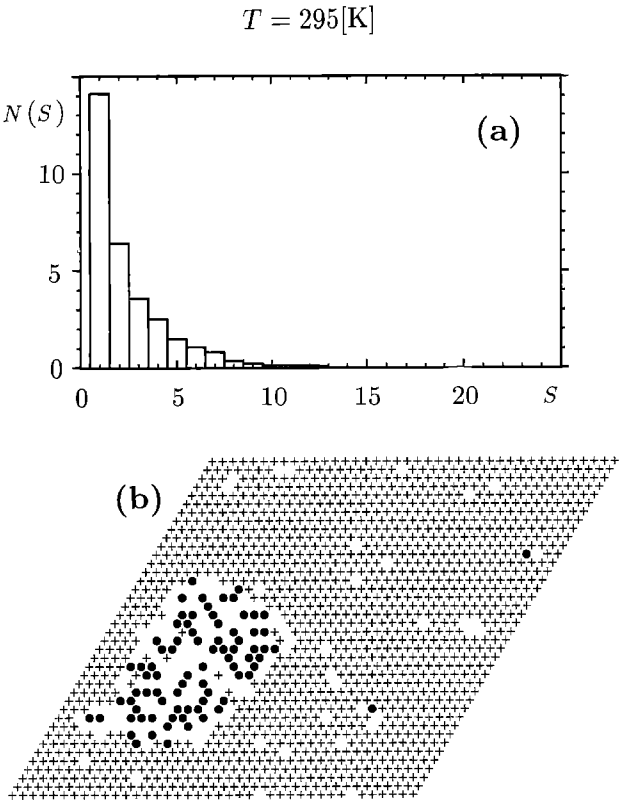

Fig. 5. *Case B* (**a**): Protein cluster size distribution on a lattice of 40×40 sites, 80 of which are single-site protein-like impurities with a hydrophobic length of 12 Å. The data are given for the temperature $T_1 = 295$ K. The lipid-protein interaction parameters are $\gamma_{mis} = 0.01 \times 10^{-13}$ erg Å^{-2} and $v_{vdW} = 0.005 \times 10^{-13}$ erg Å^{-2}. (**b**) Snapshot of a typical microconfiguration of the lattice at T_1

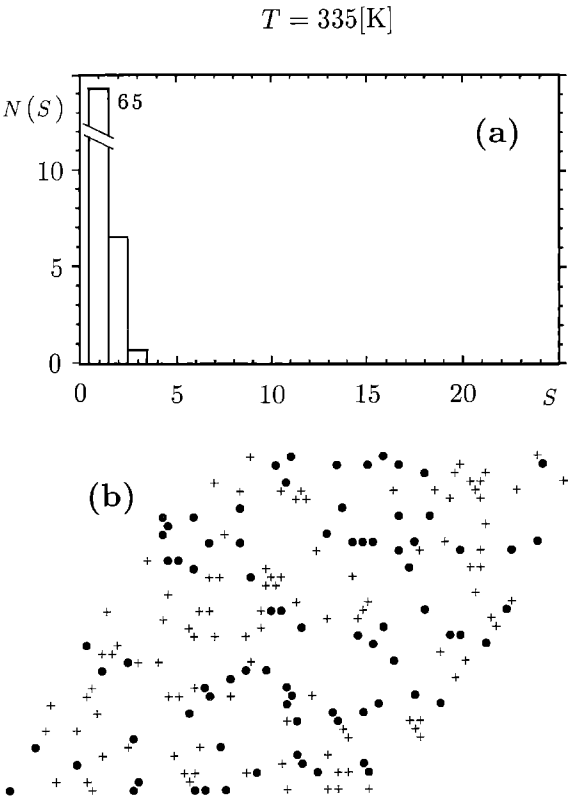

Fig. 6. *Case B* (**a**): Protein cluster size distribution on a lattice of 40×40 sites, 80 of which are single-site protein-like impurities with a hydrophobic length of 12 Å. The data are given for the temperature $T_3 = 335$ K. The lipid-protein interaction parameters are $\gamma_{mis} = 0.01 \times 10^{-13}$ erg Å^{-2} and $v_{vdW} = 0.005 \times 10^{-13}$ erg Å^{-2}. (**b**) Snapshot of a typical microconfiguration of the lattice at T_3

Case C: $d_P = 12$ Å, $v_{vdW} = 0.03 \times 10^{-13}$ erg Å^{-2} (Figs. 7–9)

The further increase in the direct van der Waals-like attractive interaction between lipids and proteins causes a slight shrink of the phase separation region compared to *Cases A* and *B* as seen in Fig. 7. However, only the phase boundary between the gel phase and the coexistence region has changed significantly indicating an increased relative solubility of the proteins in the gel phase. In the phase separation region, the proteins are mainly dissolved in the fluid regions of the lipid matrix. The results from the simulations at all three temperatures T_1, T_2, and T_3 show that the proteins do not have the tendency to cluster, cf. Figs. 8 a and b, but remain isolated from one another in contrast to *Cases A* and *B*. Figure 9 a and b shows snapshots of microconfigurations typical of the temperatures in Fig. 8 a and b.

These results indicate how the existence (in this case at low temperatures) of a large mismatch between lipid and protein hydrophobic thicknesses (similar to that in *Cases A* and *B*) is not sufficient alone to induce protein aggregation if the attractive lipid-protein interaction is sufficiently strong. On the other hand, a comparison between the results of *Cases A*, *B*, and *C*, where a short protein length is considered ($d_P = 12$ Å $\approx d_{10}$), suggests that increasing the strength of the van der Waals-like lipid-protein interaction does not change the phase dia-

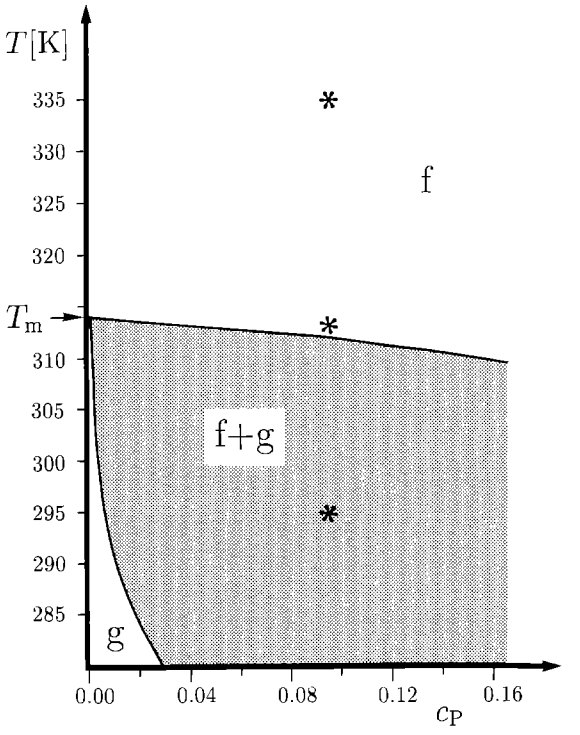

Fig. 7. *Case C:* Phase diagram in temperature, T, vs. protein concentration, c_P, for a mixture of lipids and single-site proteins with a hydrophobic length of 12 Å. The lipid-protein interaction parameters are $\gamma_{mis} = 0.01 \times 10^{-13}$ erg Å^{-2} and $v_{vdW} = 0.03 \times 10^{-13}$ erg Å^{-2}

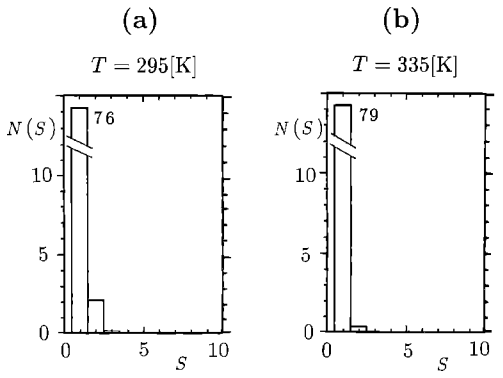

Fig. 8a, b. *Case C:* Protein cluster size distribution on a lattice of 40×40 sites, 80 of which are single-site protein-like impurities with a hydrophobic length of 12 Å. The data are given for the temperature $T_1 = 295$ K (**a**) and $T_3 = 335$ K (**b**). The lipid-protein interaction parameters are $\gamma_{mis} = 0.01 \times 10^{-13}$ erg Å^{-2} and $v_{vdW} = 0.03 \times 10^{-13}$ erg Å^{-2}

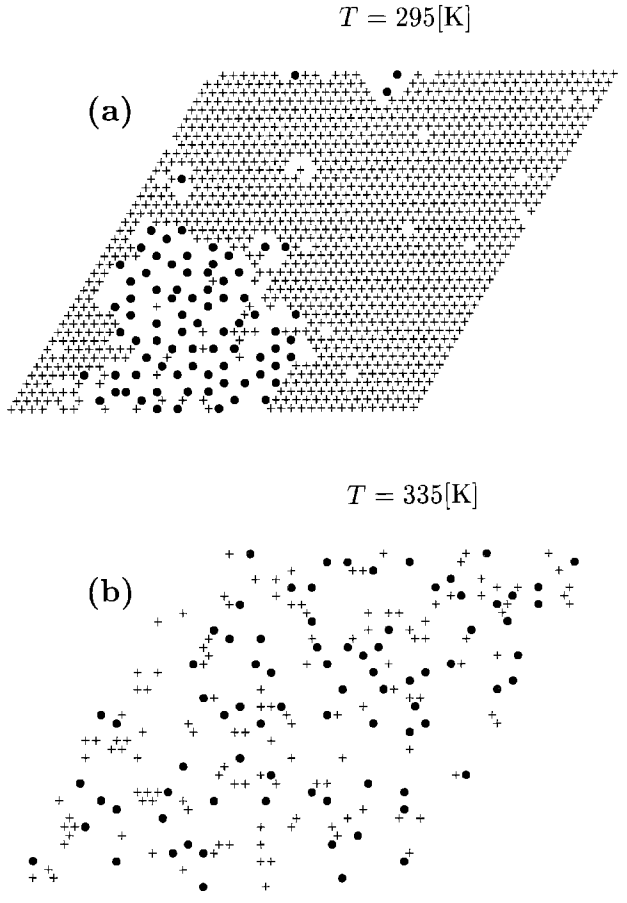

Fig. 9a, b. *Case C:* Snapshot of typical microconfigurations of a lattice with 40×40 sites, 80 of which are single-site protein-like impurities with a hydrophobic length of 12 Å. The snapshots refer to the temperatures T_1 (**a**) and T_3 (**b**). The lipid-protein interaction parameters are $\gamma_{mis} = 0.01 \times 10^{-13}$ erg Å^{-2} and $v_{vdW} = 0.03 \times 10^{-13}$ erg Å^{-2}

gram significantly. The proteins prefer to be dissolved in the fluid regions of the system where their concentration is only little affected by the changes in v_{vdW}. However, since the solubility in the fluid bilayer phase depends on v_{vdW}, the probability to form protein aggregates increases

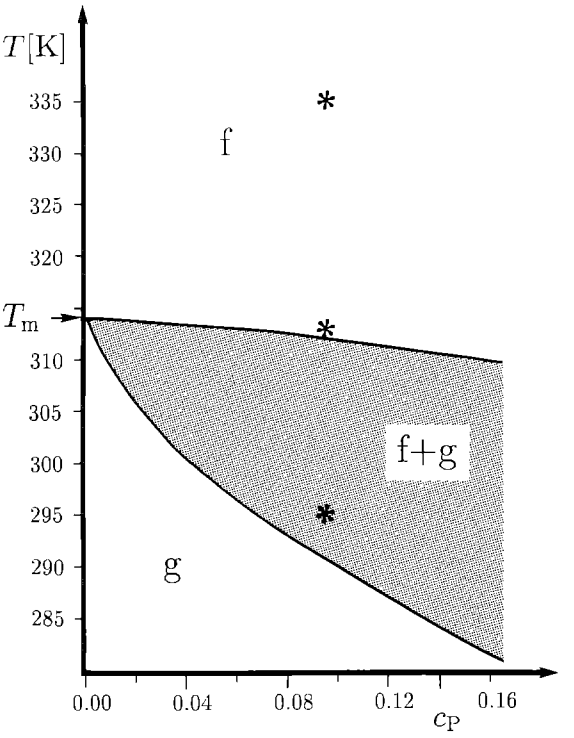

Fig. 10. *Case D:* Phase diagram in temperature, T, vs. protein concentration, c_P, for a mixture of lipids and single-site proteins with a hydrophobic length of 15 Å. The lipid-protein interaction parameters are $\gamma_{mis} = 0.01 \times 10^{-13}$ erg Å^{-2} and $v_{vdW} = 0.005 \times 10^{-13}$ erg Å^{-2}

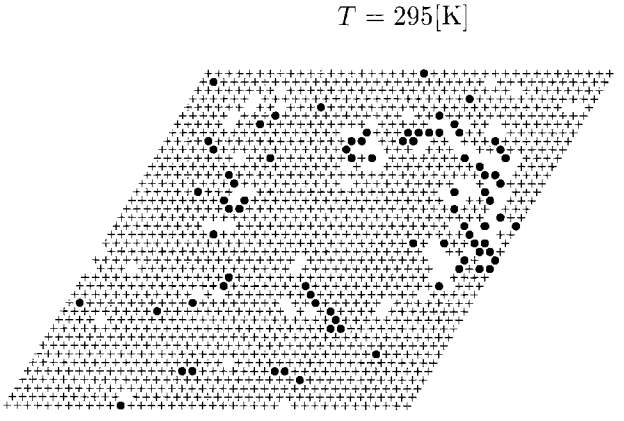

Fig. 11. *Case D:* Snapshot of typical microconfigurations of a lattice with 40×40 sites, 80 of which are single-site protein-like impurities with a hydrophobic length of 15 Å. The snapshots refers to the temperatures T_1. The lipid-protein interaction parameters are $\gamma_{mis} = 0.01 \times 10^{-13}$ erg Å^{-2} and $v_{vdW} = 0.005 \times 10^{-13}$ erg Å^{-2}

for decreasing v_{vdW}, as can be seen from a comparison between Figs. 3a, 5a and 8a at low temperatures or between Figs. 4b, 6a and 8b at high temperatures.

Case D: $d_P = 15$ Å, $v_{vdW} = 0.005 \times 10^{-13}$ erg Å^{-2} (Figs. 10, 11)

In Fig. 10 is shown the phase diagram for this system. For temperatures below T_m, the decrease (compared to

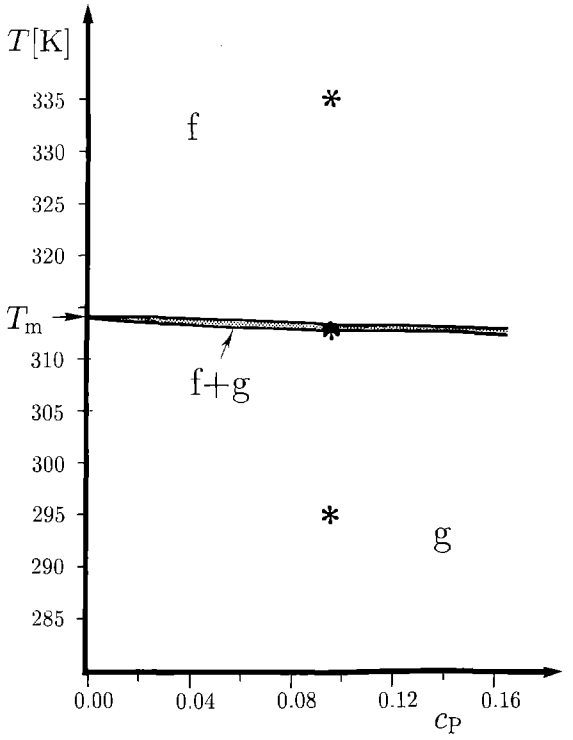

Fig. 12. *Case E:* Phase diagram in temperature, T, vs. protein concentration, c_P, for a mixture of lipids and single-site proteins with a hydrophobic length of 15 Å. The lipid-protein interaction parameters are $\gamma_{mis}=0.01\times10^{-13}$ erg Å^{-2} and $v_{vdW}=0.03\times10^{-13}$ erg Å^{-2}

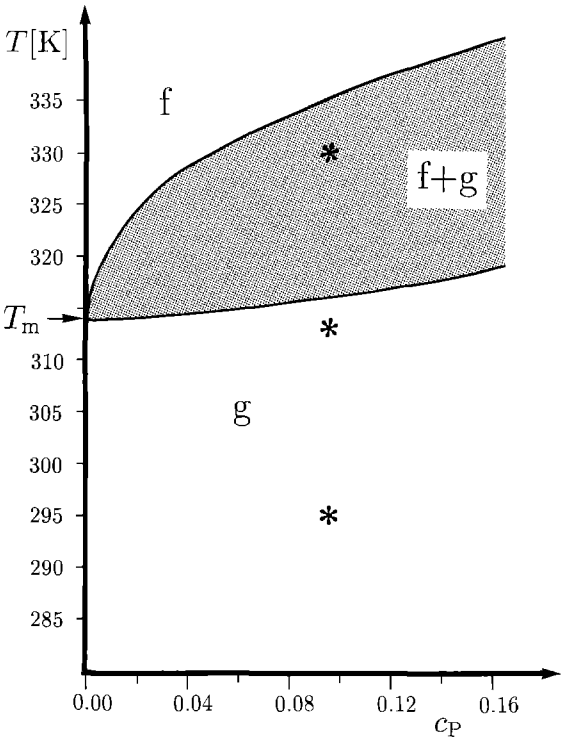

Fig. 13. *Case F:* Phase diagram in temperature, T, vs. protein concentration, c_P, for a mixture of lipids and single-site proteins with a hydrophobic length of 18 Å. The lipid-protein interaction parameters are $\gamma_{mis}=0.01\times10^{-13}$ erg Å^{-2} and $v_{vdW}=0.03\times10^{-13}$ erg Å^{-2}

Case B) in the mismatch between the lipid and protein hydrophobic thicknesses (See Fig. 1) is seen to produce a further narrowing of the phase separation region. At $T<T_m$, a substantial fraction of the proteins is now dissolved also in the gel phase, cf. Fig. 11. For the chosen protein concentration $c_P=0.095$, the data from the simulations at T_2 and T_3 do not differ substantially from those of *Case B*. At T_1 the number of isolated proteins is higher than in *Case B* due to the increase in the protein solubility in the gel regions of the bilayer. This is confirmed by the snapshot of a typical microconfiguration of the lattice at T_1 shown in Fig. 11.

Case E: $d_P=15$ Å, $v_{vdW}=0.03\times10^{-13}$ erg Å^{-2} (Fig. 12)

For this larger value of v_{vdW} the phase diagram of the mixture has a very narrow phase separation region as seen in Fig. 12. The results of the simulations indicate that, for the three considered temperatures T_1, T_2 and T_3, the proteins remain isolated from one another. This fact is not surprising if one considers the results discussed for *Case C* ($d_P=12$ Å): at low temperatures ($T\ll T_m$), the effective strength of the van der Waals-like lipid-protein interaction is the same as in *Case C*, but as soon as the temperature increases, the strength increases even further than in *Case C*, because of the increase in the contact region between the lipid chains and the protein hydrophobic surface. Therefore the proteins do not tend to aggregate no matter what the phase of the system is.

From a comparison between the results discussed for *Cases D* and *E* it is concluded that, for proteins with a hydrophobic length of 15 Å the formation of small clusters in the fluid regions of the lattice below T_m, and at high temperatures is mainly governed by the strength of the van der Waals-like lipid-protein interaction.

Case F: $d_P=18$ Å, $v_{vdW}=0.03\times10^{-13}$ erg Å^{-2} (Figs. 13, 14)

For a mixture of lipids and proteins with a hydrophobic length comparable to the one of the lipid chains in the gel phase, the phase diagram has a broad phase separation region which lies above the pure lipid transition temperature as shown in Fig. 13. This is in accordance with the general predictions of the mattress model (Mouritsen and Bloom 1984). The results from the simulations at T_1, T_2, T_3, and at $T=330$ K indicate that the proteins tend to remain isolated at all temperatures, cf. Fig. 14. The reason for this is that in the gel phase the protein is closely matched to the unperturbed lipid bilayer thickness, cf. Fig. 1. In the fluid phase and the fluid-phase regions of the coexistence region the proteins also remain dispersed despite the larger mismatch simply because the effective strength of the lipid-protein interaction is the same as in the cases with $d_P=12$ Å and 15 Å which did not lead to phase separation.

A comparison between the results obtained for the *Cases C*, *E* and *F* (proteins with a hydrophobic length of 12, 15 and 18 Å, respectively) shows that for the chosen interaction parameter, $v_{vdW}=0.03\times10^{-13}$ erg Å^{-2}, the proteins do not tend to aggregate in the fluid phase even though the mismatch is increased substantially.

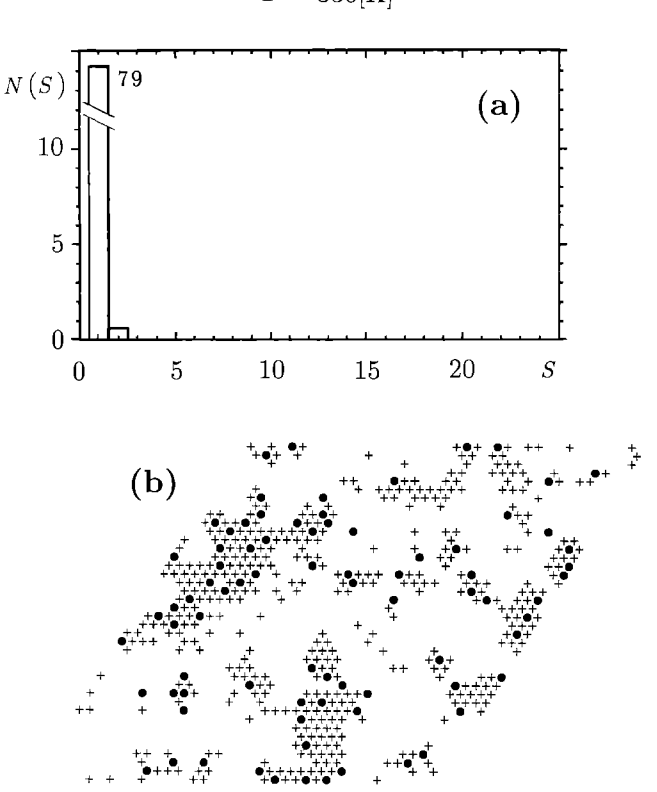

Fig. 14. *Case F* (**a**): Protein cluster size distribution on a lattice of 40×40 sites, 80 of which are single-site protein-like impurities with a hydrophobic length of 18 Å. The data are given for the temperature $T = 330$ K. The lipid-protein interaction parameters are $\gamma_{mis} = 0.01 \times 10^{-13}$ erg Å^{-2} and $\nu_{vdW} = 0.03 \times 10^{-13}$ erg Å^{-2}. (**b**) Snapshot of a typical microconfiguration of the lattice at $T = 330$ K

Discussion and conclusion

Several factors may control the lateral distribution of proteins in the lipid membrane plane. Among these the following are of major importance *a*) The protein concentration c_P; the higher c_P is, the higher is the probability for a protein to be next to another protein and hence to form an aggregate. *b*) The temperature; the higher the temperature is, the higher is the effect of the entropy which will tend to randomize the protein distribution. *c*) The lipid-protein interactions and the lipid-mediated protein-protein interactions. *d*) The direct protein-protein interactions which may be of long range due to extramembrane moieties.

We have in this paper been concerned with the factors *b*) and *c*). By means of a microscopic interaction model of a lipid-protein mixture we have performed a systematic study to investigate the relative importance for protein aggregation of different contributions to the lipid-protein interactions, specifically the attractive lipid-protein hydrophobic contact interaction and the repulsive interaction due to a possible mismatch between lipid bilayer and protein hydrophobic thicknesses. Our results suggest that the formation of protein aggregates in the membrane plane may be controlled by the strength of the direct van der Waals-like lipid-protein interaction. In contrast, it is found that a mismatch may not alone be the reason for protein aggregation: depending on the van der Waals-like interaction between lipid and protein hydrophobic contact, the proteins may still remain dispersed in the fluid phospholipid bilayer, even if the mismatch between the lipid and protein bilayer thicknesses is as high as 12 Å.

This result is consistent with the freeze-fracture work of Lewis and Engelman (1983) who studied the effect of fluid lipid bilayer thicknesses on the planar organization of the transmembane protein bacteriorhodopsin. These authors found that, well above the pure lipid transition temperature, a surprisingly large difference between protein and lipid hydrophobic thicknesses could be accommodated without inducing aggregation of the proteins. Only for very thin bilayers (from 10 to 14 Å thinner than the protein hydrophobic length) did they find signs of protein aggregation. That the hydrophobic mismatch is a major determinant of the phase equilibria has been demonstrated by calorimetric and nuclear magnetic resonance studies of the interaction of α-helical amphiphilic model polypeptides of different hydrophobic stretch with phospholipid bilayer membranes of different thicknesses (Huschilt et al. 1985, Zhang et al. 1990). Our work suggests that interesting cases to consider experimentally would be cases where the lipid acyl chain is too short ($d_P > d_1$) or too long ($d_P < d_{10}$) to match the hydrophobic surface of the proteins. For these cases, the cost in free energy needed to keep a hydrophobic surface exposed to the water is presumably very high and protein aggregation might be favoured despite the loss of entropy upon aggregation.

The cases considered in the present paper indicate that, when the value of the lipid-protein interaction parameter ν_{vdW} is sufficiently small, small clusters may also form in the fluid region of the phase diagram just above the phase boundary due to dynamic aggregation induced by the lipid-density fluctuations (see e.g. *Cases B* and *D* at $T = 313$ K). This is a highly non-trivial effect caused by the dramatic density fluctuations accompanying the main transition. The density fluctuations manifest themselves microscopically as formation of lipid gel domains in the fluid phase close to the transition (Mouritsen and Zuckermann 1985). The lipid domains are characterized by a coherence length which is related to the distance over which lipid-mediated protein-protein attractive forces are operative (Jähnig 1981; Sperotto and Mouritsen 1990). Hence by this mechanism lipid fluctuations can induce dynamic protein aggregation which should be most pronounced close to the phase boundaries.

It appears from our calculations that the mismatch interaction only has a marginal effect on the protein aggregation (except for the lipid-fluctuation-induced dynamic aggregation near the phase boundaries). Moreover, the attractive lipid-protein interactions tend to keep the proteins apart by 'spacing' them with lipids. Such 'spacer' lipids are bound in the sense that they are dynamically trapped, see e.g. Fig. 9a. Hence the direct lipid-protein van-der Waals-like interactions studied in this paper tend to reduce the degree of protein aggregation. In

fact all of the cases studied here have protein cluster size distributions which are less polydisperse than those of a truly random distribution of proteins at the same (local) concentration. The interactions of the model in (2) simply counteract the entropic forces. By focusing on a model without direct protein-protein interactions we have therefore been able to isolate the effects of purely lipid-facilitated protein aggregation. It is important to know the nature of these effects before more realistic and complicated models involving long-range direct protein-protein interactions are invoked.

The results presented in this work were derived in the case of small proteins. They should therefore be immediately applicable to mixtures of lipid membranes with simple α-helical polypeptides. However, the general picture found is expected to apply also for larger and more realistic protein sizes. Larger proteins are known to induce larger lipid-mediated attractive protein-protein interactions (Sperotto and Mouritsen 1990) which would enhance the tendency for aggregation, in particular close to the phase boundaries where the coherence length of the lipid-mediated force is maximal. Moreover, for larger proteins a further complication is that the aggregates would be complexes of proteins with lipids trapped in the interstitial regions between several proteins (Pink 1984).

The model used in the present work does not consider the direct van der Waals-like protein-protein interactions which may be responsible for the formation of short-time protein aggregates in the membrane. Furthermore the model is based both on an assumption of smoothness of the protein hydrophobic surface as well as on the hypothesis that, due to the hydrophobic effect, a mismatch interaction is acting between a lipid and a protein when their hydrophobic surfaces do not match. In the case where the assumption of 'smoothness' is no longer valid, the mismatch hypothesis is probably valid only if the proteins interact with gel-like lipid hydrocarbon chains, but it may fail for the case of fluid-like chains, which may easily fit to the rough surface of the protein without requiring a large cost in elastic energy. In this case different values of the interaction parameter γ_{mis} should be used for proteins interacting with a lipid chain in a fluid or in a gel-like state.

The mean-field approximation method and the Monte Carlo simulations have been used here as complementary techniques. The mean-field calculations provide an approximate phase diagram which serves as a useful guide to choose model parameters. The phase diagram is difficult to obtain from Monte Carlo calculations in the canonical ensemble (Mouritsen 1990). On the other hand the simulations give access to microscopic features of the system in each phase and hence provide the lateral organization of the membrane components and the state of aggregation of the proteins. Admittedly our model of lipid-protein interactions in lipid membranes is very crude with a number of details missing. However, at the present stage of theoretical modelling it is important first of all to identify which physical mechanisms are responsible for the general behaviour of membrane systems. The work presented in this paper is an attempt in this direction.

Acknowledgements. This work was supported by the Danish Natural Science Research Council under grant J.nr. 5.21.99.72 and 11-7785.

Appendix: Mean-field theory and phase diagram

The phase behaviour of a lipid-protein mixture is governed by its free energy which, from statistical mechanics, can be written in terms of the model Hamiltonian $\mathscr{H}$ and an equilibrium distribution function, ϱ

$$F = \mathrm{Tr}(\varrho\,\mathscr{H}) + k_{\mathrm{B}}\,T\,\mathrm{Tr}[\varrho\,\ln(\varrho)], \tag{3}$$

where the first term on the right-hand side is the internal energy of the system and the second term the entropy. k_{B} is the Boltzmann constant. In the mean-field approximation the lattice sites are considered statistically independent and the distribution function ϱ can therefore be written as a product of single-site distribution functions ϱ_i,

$$\varrho = \prod_{i=1}^{N} \varrho_i, \quad \varrho_i \equiv \varrho_1 \quad \forall i,$$

where

$$\mathrm{Tr}(\varrho_i) = 1, \tag{4}$$

Furthermore, the occupation variables $\mathscr{L}_m$ *and* L_{P} in $\mathscr{H}$, Eq. (2) are replaced by their average values $\langle \mathscr{L}_m \rangle$ and $\langle L_{\mathrm{P}} \rangle$.

The distribution function ϱ is now calculated by minimizing F with respect to ϱ_1, under the constraint Eq. (4), which leads to

$$\varrho_1 = \frac{\mathrm{e}^{-\beta\mathscr{H}^{\mathrm{MF}}}}{\mathrm{Tr}(\mathrm{e}^{-\beta\mathscr{H}^{\mathrm{MF}}})}, \tag{5}$$

where $\beta = (k_{\mathrm{B}}\,T)^{-1}$. $\mathscr{H}^{\mathrm{MF}}$ is the mean-field Hamiltonian which can be expressed as a linear function of the occupation variables $\mathscr{L}_m$ and L_{P}

$$\mathscr{H}^{\mathrm{MF}} = N\left(\sum_m E_m^{\mathrm{MF}}\,\mathscr{L}_m + E_{\mathrm{P}}^{\mathrm{MF}}\,L_{\mathrm{P}}\right) \tag{6}$$

where

$$E_{\mathrm{P}}^{\mathrm{MF}} = \Pi\,A_{\mathrm{P}} + \gamma_{\mathrm{mis}}\,\varrho_{\mathrm{P}} \sum_m |d_m - d_{\mathrm{P}}| \langle \mathscr{L}_m \rangle + - v_{\mathrm{vdW}}\,\varrho_{\mathrm{P}} \sum_m \min(d_m, d_{\mathrm{P}}) \langle \mathscr{L}_m \rangle,$$

$$E_m^{\mathrm{MF}} = (E_m + \Pi\,A_m) - J_0\,z\,I_m \sum_n I_n \langle \mathscr{L}_m \rangle + + [\gamma_{\mathrm{mis}}\,\varrho_{\mathrm{P}}\,|d_m - d_{\mathrm{P}}| - v_{\mathrm{vdW}}\,\varrho_{\mathrm{P}}\,\min(d_m, d_{\mathrm{P}})] \langle L_{\mathrm{P}} \rangle.$$

N is the total number of lattice sites and z is the coordination number ($z = 6$). It is now possible, with the use of Eqs. (5) and (6), to calculate the mean values of the ten occupation variables, $\mathscr{L}_m$, $m = 1, \ldots 10$, from a set of ten self-consistent equations

$$\langle \mathscr{L}_m \rangle = \frac{\mathrm{Tr}(\mathscr{L}_m\,\mathrm{e}^{-\beta\mathscr{H}^{\mathrm{MF}}})}{\mathscr{Z}} = \frac{D_m\,\mathrm{e}^{-\beta E_m^{\mathrm{MF}}}}{\mathscr{Z}}, \quad m = 1, \ldots 10,$$

where $\mathscr{Z}$ is the single-site partition function. Replacing $\langle L_P \rangle$ by the fraction of lattice sites occupied by the proteins, x_P, the single-site partition function becomes

$$\mathscr{Z} = \frac{1}{(1-x_P)} \sum_{m=1}^{10} D_m \, e^{-\beta E_m^{MF}}. \tag{7}$$

For single-site proteins, the protein molar concentration, c_P, is related to x_P by

$$\langle \mathscr{L}_m \rangle \equiv x_P = \frac{c_P}{2 - c_P}, \tag{8}$$

accounting for the fact that a lipid molecule occupies two lattice sites. From the knowledge of $\langle \mathscr{L}_m \rangle$ it is now possible to give the full expression for the mean-field free energy *per* site

$$\tilde{F} = \tilde{U} - T\,\tilde{S}, \tag{9}$$

where

$$\tilde{U} = \sum_m (E_m + \Pi A_m) \langle \mathscr{L}_m \rangle - \frac{J_0}{2} \left(\sum_m I_m \langle \mathscr{L}_m \rangle \right)^2 + \\ + \left[\gamma_{mis} \left(\frac{\varrho_P}{z} \right) \sum_m |d_m - d_P| - v_{vdW} \left(\frac{\varrho_P}{z} \right) \sum_m \min(d_m, d_P) \right] \\ \cdot x_P + \Pi A_P x_P$$

$$\tilde{S} = -k_B T \left[\sum_m \langle \mathscr{L}_m \rangle \ln \left(\frac{\langle \mathscr{L}_m \rangle}{D_m} \right) - x_P \ln x_P \right],$$

and $\tilde{S}$ is the entropy of ideal mixing.

The range of protein concentration and temperature over which two phases coexist (the phase separation region) is a two-phase region of the phase diagram which is constructed as follows (Lee 1977): for a given temperature and protein molar concentration c_P, the function

$$\tilde{F}(c_P^{(1)}, c_P^{(2)}, c_P) = \frac{(c_P^{(2)} - c_P)\,\tilde{F}(c_P^{(1)}) + (c_P - c_P^{(1)})\,\tilde{F}(c_P^{(2)})}{(c_P^{(2)} - c_P^{(1)})} \tag{10}$$

is minimized with respect to the two protein concentrations $c_P^{(1)}$ and $c_P^{(2)}$, which are chosen in such a way that $c_P^{(1)} \leq c_P$ and $c_P^{(2)} \geq c_P$. The values of $c_P^{(1)}$ and $c_P^{(2)}$ for which the function in Eq. (10) has a minimum determine either the concentration of protein in two different phases (if $c_P^{(1)} \neq c_P$ and $c_P^{(2)} \neq c_P$) or assure that only one phase is present (if $c_P^{(1)} = c_P^{(2)} = c_P$).

References

Abney JR, Owicki JC (1985) Theories of protein-lipid and protein-protein interactions in membranes. In: Watts A, de Pont JJHHM (eds) Progress in protein-lipid interactions. Elsevier, Amsterdam, pp 1–60

Abney JR, Braun J, Owicki JC (1987) Lateral interactions among membrane proteins. Implications for the organization of gap junctions. Biophys J 52:441–454

Barion A, Bienvenue A, Devaux F (1979) Spin-label studies of protein-protein interactions in retinal rod outer segement membranes. Saturation transfer electron paramagnetic resonance spectroscopy. Biochemistry 18:1151–1155

Braun J, Abney JR, Owicki JC (1987) Lateral interactions among membrane proteins. Valid estimates based on freeze-fracture electron microscopy. Biophys J 52:427–439

Caillé A, Pink DA, de Verteuil F, Zuckermann MJ (1980) Theoretical models of quasi-two-dimensional mesomorphic monolayers and membrane bilayers. Can J Phys 58:581–611

Carruthers A, Melchior DL (1986) How bilayer lipids affect membrane protein activity. Trends Biochem Sci 11:331–335

Huschilt JC, Hodges RS, Davis JH (1985) Phase equilibria in an amphiphilic peptide-phospholipid model membrane by ^2H nuclear magnetic resonance spectroscopy Biochemistry 24:1377–1385

Jähnig F (1981) Critical effects from lipid-protein interactions in membranes. I. Theoretical description. Biophys J 36:329–345

Lee AG (1977) Lipid phase transitions and phase diagrams. II. Mixtures involving lipids. Biochim Biophys Acta 472:285–344

Lewis BA, Engelman DM (1983) Bacteriorhodopsin remains dispersed in fluid phospholipid bilayers over a wide range of bilayer thicknesses. J Mol Biol 166:203–210

Lookman T, Pink DA, Grundke EW, Zuckermann MJ, de Verteuil F (1982) Phase separation in lipid bilayers containing integral proteins. Computer simulation studies. Biochemistry 21:5593–5601

MacDonald AL, Pink DA (1987) Thermodynamics of glycophorin in phospholipid bilayer membranes. Biochemistry 26:1909–1917

Marčelja S (1974) Chain ordering in liquid crystals. II. Structure of bilayer membranes. Biochim Biophys Acta 367:165–176

Marčelja S (1976) Lipid-mediated protein-protein interaction in membranes. Biochim Biophys Acta 455:1–7

McElhaney RN (1982) Effects of membrane lipids on transport and enzymatic activities. In: Razin S, Rottem S (eds) Current topics in membranes and transport, vol 17. Academic Press, New York, pp 317–380

Metzger H, Ishizaka T (1982) Transmembrane signaling by receptor aggregation: the mast cell receptor for IgE as a case study. Fed Proc 41:7

Mouritsen OG (1990) Computer simulation of cooperative phenomena in lipid membranes. In: Brasseur R (ed) Molecular description of membrane components by computer-aided conformational analysis, vol 1. CRC Press, Boca Raton, pp 3–83

Mouritsen OG, Bloom M (1984) Mattress model of lipid-protein interactions in membranes. Biophys J 46:141–153

Mouritsen OG, Zuckermann MJ (1985) Softening of lipid bilayers. Eur Biophys J 12:75–86

Mouritsen OG, Boothroyd A, Harris R, Jan N, Lookman T, MacDonald L, Pink DA, Zuckermann MJ (1983) Computer simulation of the main gel-fluid transition of lipid bilayers. J Chem Phys 79:2027–2041

Pearson LT, Chan SI, Lewis BA, Engelman DM (1983) Pair correlation functions of bacteriorhodopsin in model bilayers. Biophys J 43:167–174

Peschke J, Riegler J, Möhwald H (1987) Quantitative analysis of membrane distortions induced by mismatch of protein and lipid hydrophobic thickness. Eur Biophys J 14:385–391

Pink DA (1984) Theoretical studies of phospholipid bilayers and monolayers. Perturbing probes, monolayer phase transition, and computer simulations of lipid-protein bilayers. Can J Biochem Cell Biol 62:760–777

Pink DA, Chapman D (1979) Protein-lipid interactions in bilayer membranes: a lattice model. Proc Natl Acad Sci USA 76:1542–1546

Pink DA, Hamboyan H (1990) Effect of integral proteins upon bilayer permeability to ions. Eur Biophys J 18:245–251

Pink DA, Green T, Chapman D (1980) Raman scattering in bilayers of saturated phosphatidylcholines and cholesterol. Experiment and theory. Biochemistry 19:349–356

Quinn PJ, Chapman D (1980) The dynamics of membane structure. CRC Crit Rev Biochem 8:1–117

Riegler J, Möhwald H (1986) Elastic interactions of photosynthetic reaction center proteins affecting phase transitions and protein distributions. Biophys J 49:1111–1118

Sackmann E (1984) Physical basis of trigger processes and membrane structures. In: Biological membranes, vol 5. Academic Press, London, pp 105–143

Sadler DM, Worcester DL (1982) Neutron scattering studies of photosynthetic membranes in aqueous dispersion. J Mol Biol 159: 485–499

Sadler DM, Rivas E, Gulik-Krzywicki T, Reiss-Husson F (1984) Measurements of membrane thickness by small-angle neutron scattering of suspensions: results for reconstituted *Rhodopseudomonas sphaeroides* reaction-center protein and for lipids. Biochemistry 23:2704–2712

Sandermann H (1978) Regulation of membrane enzymes by lipids. Biochim Biophys Acta 515:209–237

Singer SJ, Nicolson GL (1972) The fluid mosaic model of the structure of cell membranes. Science 173:720–731

Sperotto MM, Mouritsen OG (1988) Dependence of lipid membrane phase transition temperature on the mismatch of protein and lipid hydrophobic thickness. Eur Biophys J 16:1–10

Sperotto MM, Ipsen JH, Mouritsen OG (1989) Theory of protein-induced lateral phase separation in lipid membranes. Cell Biophys 14:79–95

Sperotto MM, Mouritsen OG (1991) Monte Carlo simulation studies of lipid order parameter profiles near integral membrane proteins. Biophys J 59 (in press)

Stoeckenius W, Lozier RH, Bogomolni RA (1979) Bacteriorhodopsin and the purple membrane of halobacteria. Biochim Biophys Acta 505:215–278

Tanford C (1973) The hydrophobic effect. Formation of micelles and biological membranes. Wiley, New York

Tessier-Lavigne M, Boothroyd A, Zuckermann MJ, Pink DA (1982) Lipid-mediated interactions between intrinsic molecules in bilayer membranes. J Chem Phys 76:4587–4599

Träuble H, Haynes DH (1971) The volume change in lipid bilayer lamellae at the crystalline-liquid crystalline phase transition. Chem Phys Lipids 7:324–335

Zhang Y, Lewis RNAH, Hodges RS, McElhaney RN (1990) Calorimetric studies of the interaction of an amphiphilic model peptide with phosphatidylcholine bilayers. Biophys J 57:71a